Nonlinear Dynamics and Systems Theory, **25** (3) (2025) 288–298

A New Memristor-Based 4D Hyperchaotic System with Seven Terms and No Equilibrium Points

M. I. Kopp *

Institute for Single Crystals, NAS of Ukraine, Nauky Ave. 60, Kharkiv 61072, Ukraine

Received: October 8, 2024; Revised: May 24, 2025

Abstract: The most pressing challenge in the practical application of chaotic systems is the development of methods for encrypting information. This paper presents a new 4-dimensional (4D) memristive system that is simple, consisting of only seven terms and lacking equilibrium points, which allows it to generate hidden attractors. The paper thoroughly analyzes the system's dynamic properties, including bifurcation diagrams, Lyapunov exponents, Kaplan-York dimensions, and offset boosting analysis. Additionally, the theoretical model is validated through electronic simulation of the new two-winged chaotic system using Multisim.

Keywords: *two-wing attractors; memristor; chaotic behavior; offset boosting control; circuit implementation.*

Mathematics Subject Classification (2020): 34A34, 34D45, 70K43, 93C15.

1 Introduction

A rapidly expanding area within nonlinear circuit theory is the development of chaos generators utilizing memristors. First introduced by Chua [1], the memristor is a device that links electric charge and magnetic flux, functioning as a resistor with memory. Since then, the concept has evolved to include a broader spectrum of memristive systems. HP Laboratories achieved the first successful implementation of a memristor, using a metal-dielectric-metal structure [2]. However, significant technological challenges in memristor fabrication have led to a considerable gap between theoretical models and experimental studies. Memristors have found extensive applications in fields such as image encryption, signal processing, biosystems, and neural networks, particularly in complex neural networks [3]. Their popularity is largely due to the complex dynamics achievable in chaotic

* Corresponding author: `mailto:michaelkopp0165@gmail.com`

systems based on memristors. Numerous chaotic and hyperchaotic systems have been developed with memristors serving as nonlinear elements. Furthermore, various equivalent circuits for modeling memristor emulators have been proposed in the literature [4]. This brief literature review focuses on 4D chaotic systems that integrate memristors. Chaotic dynamical systems can be categorized into two types: those with self-excited attractors and those with hidden attractors. A self-excited attractor has a basin of attraction that intersects with the vicinity of an equilibrium point, whereas a hidden attractor's basin does not intersect with any equilibrium point's neighborhood. The concept of hidden attractors, first introduced in [5], has since sparked ongoing research in nonlinear science. As noted in [6], hidden attractors in dynamical systems are currently classified into five categories: 1) systems without equilibria, 2) equilibrium curves, 3) planes of curves, 4) equilibrium lines, and 5) stable equilibrium points.

Recently, a new 4D hyperchaos system without equilibrium point was proposed in [7]. Several researchers have developed memristor-based 4D hyperchaotic systems characterized by the absence of equilibrium points. In [8], a 4D memristive system is introduced, consisting of 12 terms, 5 of which are nonlinear. This model notably lacks equilibrium points and exhibits periodic, chaotic, and hyperchaotic behavior within specific parameter ranges. In [9], a 4D memristive system is presented that can display either no equilibrium points or an equilibrium line, depending on the control parameter. The study shows that by adjusting this parameter, the system can transition between chaotic and hyperchaotic dynamics. This nonlinear system comprises 11 terms, including 5 nonlinear ones. A simpler 4D chaotic memristor-based system, consisting of 9 terms with 2 nonlinearities and no equilibrium points, is described in [10]. An even more streamlined 4D memristive two-scroll chaotic system, containing only 7 terms and 3 nonlinearities, is introduced in [11]. This system demonstrates various complex dynamics such as offset boosting, remerging period-doubling bifurcations, and hidden extreme multistability. Furthermore, a 4D hyperchaotic hyperjerk system with a line equilibrium, composed of 7 algebraic terms and a single nonlinearity, is proposed in [12]. Interestingly, the system in [12] is based on intrinsic memristive nonlinearity, a type of nonlinearity that arises naturally from the memristor itself.

In this paper, we present a new hyperchaotic dynamical system (not a jerk system) developed by introducing nonlinearity via a memristor. Our primary motivation is to design a novel 4D hyperchaotic memristor-based system with the fewest possible terms.

2 Derivation and Key Properties of a Novel 4D Memristive Hyperchaotic System

In this section, we introduce a novel 4D memristive two-wing chaotic system comprising only seven terms. This system is based on the one introduced in [13] and is defined as follows:

$$\begin{cases} \dfrac{dx_1}{dt} = a(-x_1 + x_2), \\ \dfrac{dx_2}{dt} = -x_3\mathrm{sgn}(x_1), \\ \dfrac{dx_3}{dt} = |x_1| - 1, \end{cases} \tag{1}$$

where $|x|$ is the absolute value function and the signum function $\mathrm{sgn}(x)$ of a real number x is a piecewise function. Figure 1 displays typical two-wing butterfly attractors in various

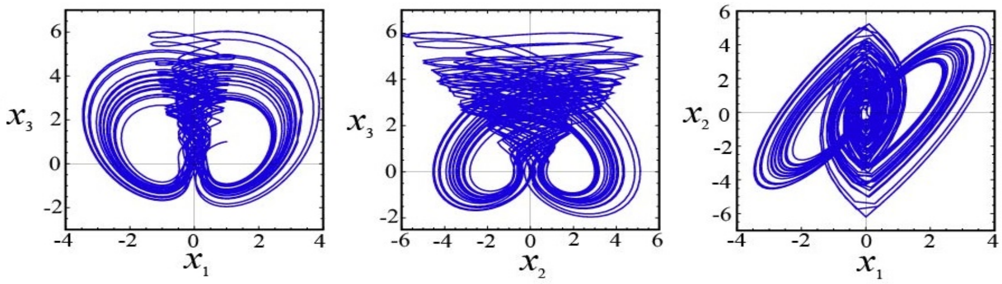

Figure 1: Plots depict the two-wing butterfly attractors of system (1) in the phase planes x_1x_3, x_2x_3, and x_1x_2, respectively.

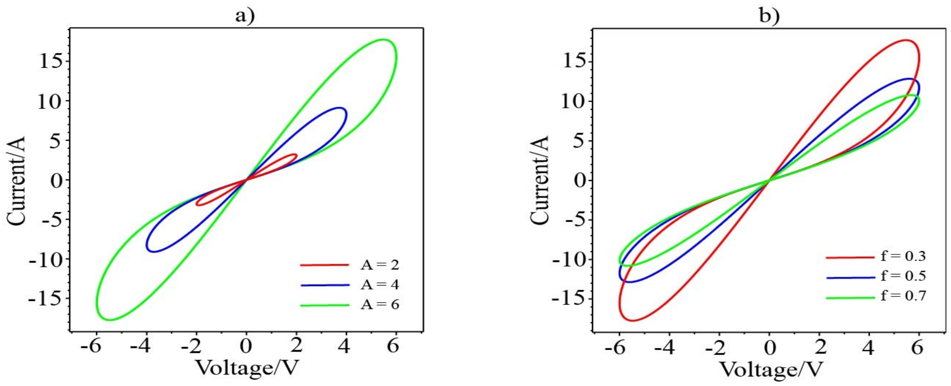

Figure 2: Simulation results of the hysteresis loop for the memductance function $W(\varphi) = 1 + 0.5|\varphi|$: a) different values of amplitude A; b) different values of frequency f.

phase planes for system (1), with parameter set at $a = 0.6$ and the initial conditions $x_1(0) = x_2(0) = x_3(0) = 1$. Using the methodology of Binouse et al. [14], we can compute all LEs:

$$LE_1 = 0.191212, \quad LE_2 \approx 0, \quad LE_3 = -0.799337,$$

and the corresponding Kaplan-Yorke (or Lyapunov) dimension $D_{KY} \approx 2.239$. We see that system (1) demonstrates chaotic behavior with one positive exponent $LE_1 > 0$.

To achieve hyperchaotic behavior, system (1) is extended to 4D by adding a state variable linked to the original system through a memristor. We use the model of an absolute memristor, specifically Bao's magnetically controlled memristor [15], described by the following equations:

$$\begin{cases} i_m = W(\varphi)u_m, \\ \frac{d\varphi}{dt} = u_m, \\ W(\varphi) = \alpha + \beta|\varphi|. \end{cases} \tag{2}$$

In the equations (2), the symbols u_m, i_m, and φ represent the input, output, and state variables of the memory device, respectively. The function φ corresponds to the magnetic flux, while α and β are constant coefficients, set to $\alpha = 1$ and $\beta = 0.5$. The graph for

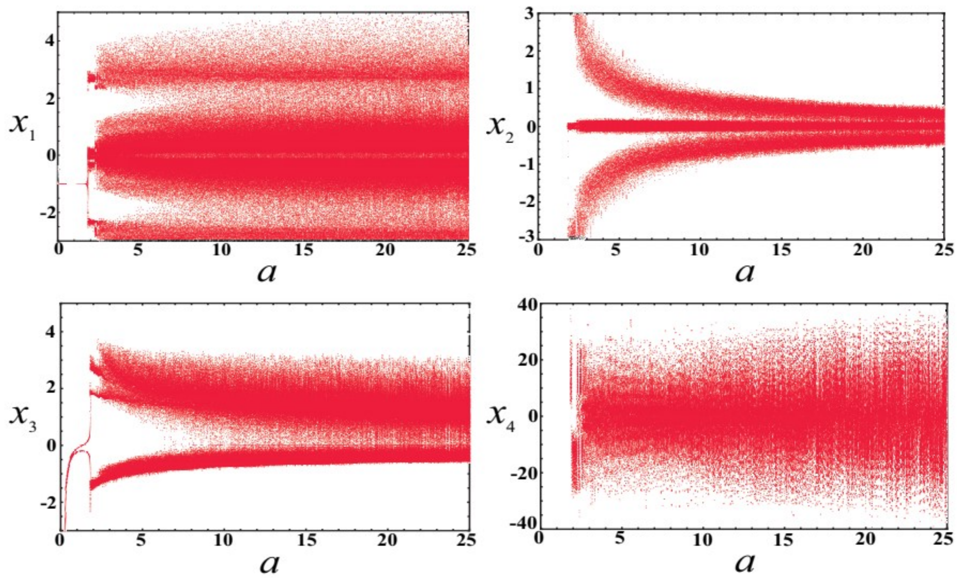

Figure 3: Bifurcation diagrams for the components x_1, x_2, x_3, x_4 of the system (3).

system (2) displays a smooth quadratic nonlinear characteristic curve passing through the origin. Driven by a sinusoidal AC voltage source $u_m = A\sin(2\pi f t)$, where A is the amplitude and f is the frequency, the memristor circuit simulation results, shown in Figure 2, reveal a current-voltage characteristic forming a closed hysteresis loop. As the frequency f increases, the area of the loop decreases, while increasing the amplitude A causes its expansion, consistent with the fundamental properties of memristors.

Integrating the expressions from (2) into the nonlinear dynamic equations (1) yields a novel set of memristor-based 4D equations:

$$\begin{cases} \dfrac{dx_1}{dt} = ax_2 - (\alpha + \beta|x_4|)x_1, \\ \dfrac{dx_2}{dt} = -x_3 \mathrm{sgn}(x_1), \\ \dfrac{dx_3}{dt} = |x_1| - 1, \\ \dfrac{dx_4}{dt} = x_1. \end{cases} \tag{3}$$

Here, instead of the notation of flux φ, we introduced a new dynamical variable x_4. As shown in (3), the system includes only seven terms. It represents the minimum number of terms needed for chaotic dynamics in a four-dimensional autonomous system, making it a rare configuration in the literature.

Let us outline some fundamental dynamic properties of the new 4D system. It is readily verifiable that system (3) exhibits symmetry with respect to the x_3-axis and remains invariant under the transformation $(x_1, x_2, x_3, x_4) \to (-x_1, -x_2, x_3, -x_4)$. To further characterize the system's behavior, we calculate its divergence as follows:

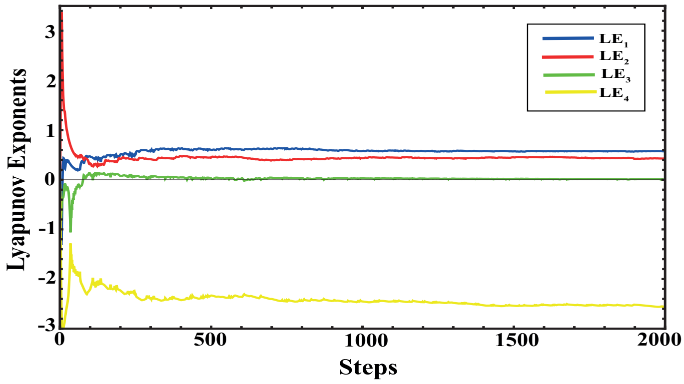

Figure 4: Lyapunov exponents for the system (3) for the parameter value $a = 21$ and initial conditions (4).

$$\frac{\partial \dot{x}_1}{\partial x_1} + \frac{\partial \dot{x}_2}{\partial x_2} + \frac{\partial \dot{x}_3}{\partial x_3} + \frac{\partial \dot{x}_4}{\partial x_4} = -(\alpha + \beta|x_4|).$$

Thus, the system (3) is dissipative for all positive values of parameters. Setting the right-hand side of system (3) to zero $\dot{x}_1 = \dot{x}_2 = \dot{x}_3 = \dot{x}_4 = 0$ yields $x_1 = 0$ from the fourth equation. Substituting this value into the third equation leads to the contradictory result $-1 = 0$, indicating that no equilibrium points exist for the system. This implies that all attractors generated by system (3) are hidden.

2.1 Bifurcation diagrams, Lyapunov exponents, and the calculation of Kaplan-Yorke dimension

In dynamic analysis, a bifurcation diagram visually represents changes in the system's state variables. We use the NDSolve function in Mathematica to solve the equations in (3) under the following initial conditions:

$$x_1(0) = x_2(0) = x_3(0) = x_4(0) = 1. \tag{4}$$

In system (3), the parameter a varies while $\alpha = 1, \beta = 0.1$ remain constant. The bifurcation diagrams in Figure 3 show the components as $a \in [0, 25]$, highlighting stable regions (distinct points), periodic, quasiperiodic, and chaotic behaviors. Examining the Lyapunov exponents provides deeper insight into the system's stability and chaotic characteristics as a changes. The dynamical behaviors of system (3) can be classified into the following categories, as detailed in Table 1. A positive LE indicates instability or chaos within the system, while a negative LE suggests a tendency toward stable equilibrium. Next, we focus on the hyperchaotic behavior of the system (3) at $a = 21$. The sum of all Lyapunov exponents is negative, confirming the dissipative nature of the system. The dynamics are illustrated in Figure 4. To assess the complexity of the attractor, we can calculate the Lyapunov or Kaplan-Yorke dimension:

$$D_{KY} = \xi + \frac{1}{|LE_{\xi+1}|} \sum_{i=1}^{\xi} LE_i = 3 + \frac{1.0041}{2.5617} \approx 3.3919, \tag{5}$$

a	Lyapunov Exponents (LE_1, LE_2, LE_3, LE_4)	Signs	Behavior
$a = 0.01$	$(\mathbf{0.0081}, -0.0148, -0.0081, -11.0423)$	$(0, -, -, -)$	Periodic
$a = 0.45$	$(\mathbf{0.0053}, \mathbf{-0.0012}, \mathbf{-0.0043}, -12.3353)$	$(0, 0, 0, -)$	Quasi − periodic 3 − torus
$a = 1$	$(\mathbf{0.0201}, \mathbf{0.0038}, -0.0165, -8.3231)$	$(0, 0, -, -)$	Quasi − periodic 2 − torus
$a = 1.85$	$(0.0881, \mathbf{-0.0057}, -0.0140, -3.8193)$	$(+, 0, -, -)$	Chaotic
$a = 3$	$(0.0936, \mathbf{0.0080}, \mathbf{0.0038}, -3.8193)$	$(+, 0, 0, -)$	Chaotic 2 − torus
$a = 4$	$(0.1471, \mathbf{0.0520}, -0.0986, -1.9904)$	$(+, 0, -, -)$	Chaotic
$a = 15$	$(0.4646, 0.2873, \mathbf{-0.0077}, -2.2215)$	$(+, +, 0, -)$	Hyperchaotic
$a = 21$	$(0.5702, 0.4303, \mathbf{0.0035}, -2.5617)$	$(+, +, 0, -)$	Hyperchaotic

Table 1: Lyapunov exponents for different values of the parameter a.

where ξ is determined from the conditions

$$\sum_{i=1}^{\xi} LE_i > 0 \;\Rightarrow\; \sum_{i=1}^{3} LE_i = 1.0041, \quad \sum_{i=1}^{\xi+1} LE_i < 0 \;\Rightarrow\; \sum_{i=1}^{4} LE_i = -1.5577 < 0.$$

Here, ξ denotes the number of first non-negative Lyapunov exponents. The Kaplan-Yorke dimension D_{KY} (5) is fractional and is found to be significantly higher for system (3) than for the chaotic system (1), indicating greater dynamic complexity.

2.2 Phase portraits of hidden attractors and offset boosting control

We created phase portraits and time diagrams for the hyperchaotic system (3), shown in Figure 5. Implementing system (3) in an electronic circuit is challenging because the dynamic variable x_4 exceeds the power supply limits of operational amplifiers. To address this, we transform x_4 to $x_4 = 20X_4$ and rename the other variables as $x_1 = X_1$, $x_2 = X_2$, and $x_3 = X_3$. The transformed hyperchaotic system takes the form

$$\begin{cases} \dfrac{dX_1}{dt} = 21X_2 - (1 + 2|X_4|)X_1, \\ \dfrac{dX_2}{dt} = -X_3\mathrm{sgn}(X_1), \\ \dfrac{dX_3}{dt} = |X_1| - 1, \\ \dfrac{dX_4}{dt} = 0.05X_1. \end{cases} \tag{6}$$

The transformed system (6) will be utilized to create an analog chaos generator circuit in the following section.

The offset boosting control method is commonly used in hyperchaotic systems to shift the attractor by introducing a bias. By adding a constant to specific variables, chaotic signals can be manipulated within phase space. In system (3), x_4 appears in the first equation and x_3 in the second. We can control these variables by replacing x_4 with $x_4 + m$ and x_3 with $x_3 + k$, where m and k are constants. As shown in Figure 6, modifying m transforms x_4 from a bipolar to a unipolar signal and shifts the attractor along the x_4-axis. Similar effects for x_3 are illustrated in Figure 7.

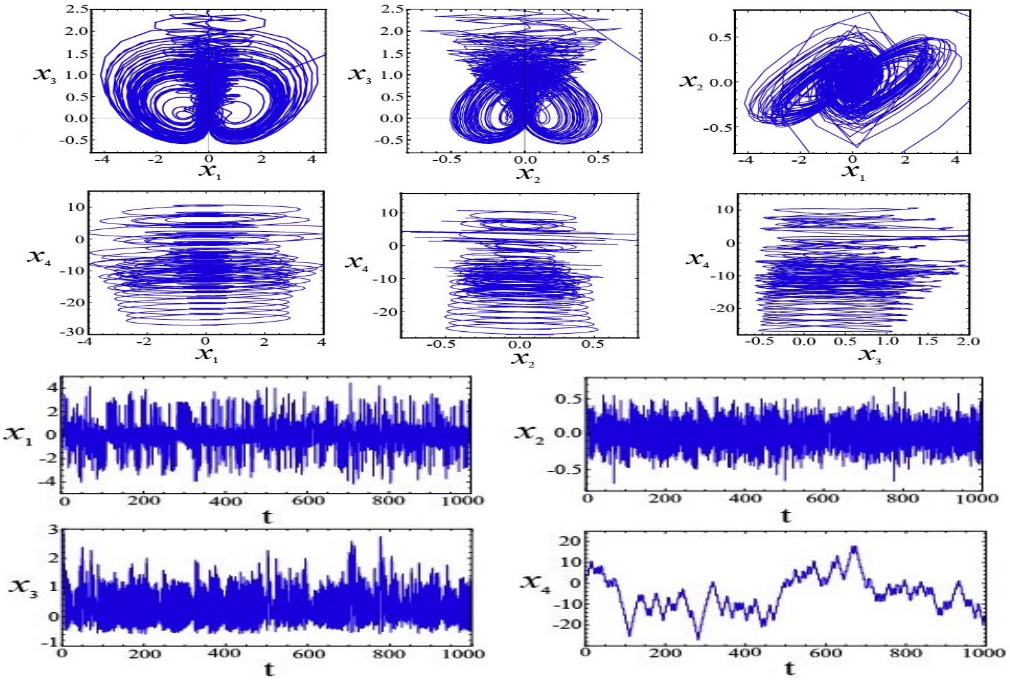

Figure 5: The upper part of the figure displays the hidden attractors of the hyperchaotic system (3) in various planes. In contrast, the lower part of the figure presents the time diagrams for the variables x_1, x_2, x_3, x_4.

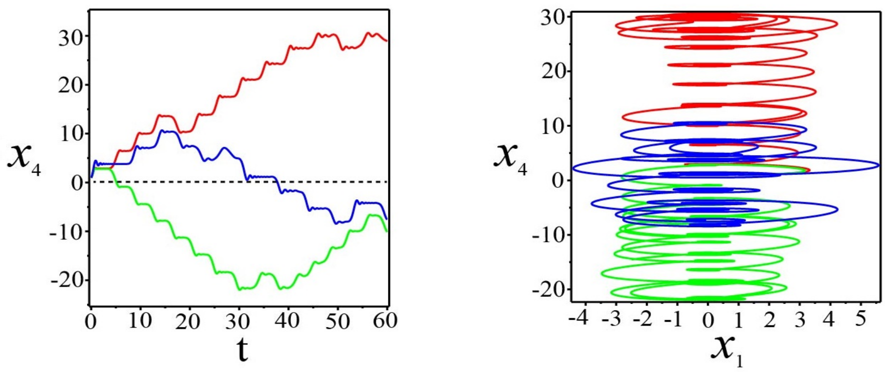

Figure 6: Signal x_4 and phase portrait in the plane x_1x_4 for different values of the offset boosting controller m: $m = 0$ (blue), $m = 30$ (green), $m = -30$ (red).

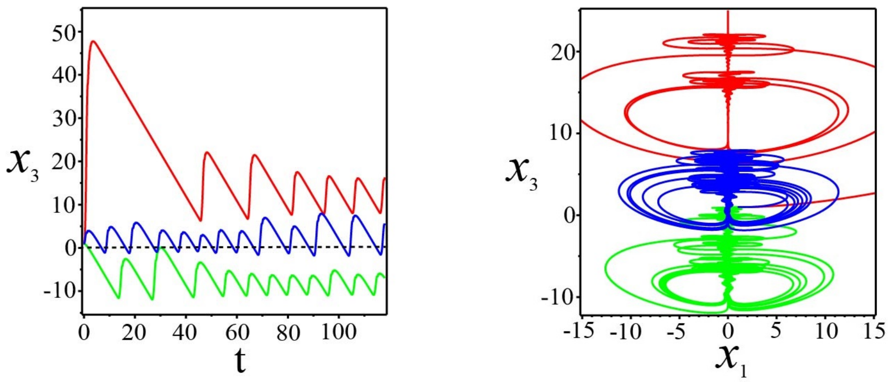

Figure 7: Signal x_3 and phase portrait in the plane x_1x_3 for different values of the offset boosting controller k: $k = 0$ (blue), $k = 10$ (green), $k = -10$ (red).

3 Electronic Circuit Design and Multisim Simulation of the New Hyperchaotic System

Based on Kirchhoff's law for electrical circuits, the electrical analog of the system (6) can be expressed as follows:

$$\begin{cases} \dfrac{d\widetilde{X}_1}{dt} = \dfrac{100\text{k}}{R_2}\widetilde{X}_2 - \left(\dfrac{100\text{k}}{R_1} + \dfrac{100\text{k}}{R_3 \cdot 10}|\widetilde{X}_4|\right)\widetilde{X}_1, \\ \dfrac{d\widetilde{X}_2}{dt} = -\dfrac{100\text{k}}{R_4 \cdot 10}\widetilde{X}_3 \text{sgn}(\widetilde{X}_1), \\ \dfrac{d\widetilde{X}_3}{dt} = \dfrac{100\text{k}}{R_5}|\widetilde{X}_1| - \dfrac{100\text{k}}{R_6}V_b, \\ \dfrac{d\widetilde{X}_4}{dt} = \dfrac{100\text{k}}{R_7}\widetilde{X}_1, \end{cases} \tag{7}$$

where $R_1 = R_5 = R_6 = 100\text{k}\Omega,\ R_2 = 4.76\text{k}\Omega,\ R_3 = 20\text{k}\Omega,\ R_4 = 10\text{k}\Omega,\ R_7 = 2\text{M}\Omega$. The analog circuit modules for the equations in system (7) are shown in Figure 8. These circuits utilize standard components such as resistors (R), capacitors (C), diodes D1-D2 (1N4001), multipliers M1-M2 (AD633), operational amplifiers A1-A21 (TL084ACN), and a supply voltage of ±15V. The constant 1 is provided by a voltage source $V_b = 1V$. Figures 8b and 8c illustrate modules that model the signum $\text{sgn}(\cdot)$ and absolute value $|\cdot|$ functions. The phase portraits in Figure 10 reveal a remarkable similarity between the Mathematica simulation results (Figure 5) and the Multisim simulation results.

4 Conclusions

In this paper, we obtained a new 4D dynamical system based on a memristor that meets the known criteria for generating hyperchaos: a) it is dissipative; b) it has a four-dimensional phase space; and c) it includes at least one nonlinear term. A new memristive four-dimensional dynamic system, derived from the five-term Lorenz equations, contains only 7 terms. This hyperchaotic system lacks equilibrium points, potentially leading to

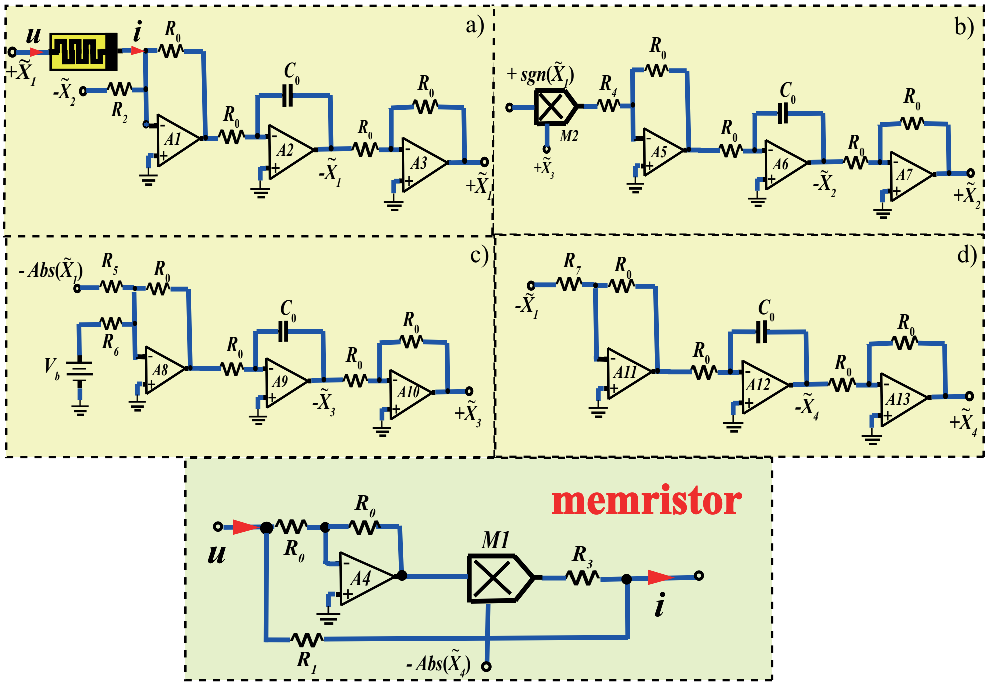

Figure 8: Circuit modules implemented based on the system of equations (5): a) $\widetilde{X}_1$, b) $\widetilde{X}_2$, c) $\widetilde{X}_3$, d) $\widetilde{X}_4$ and the memristor circuit module.

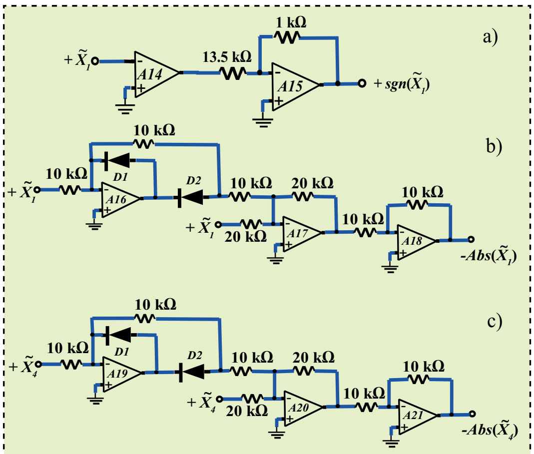

Figure 9: Schematic diagrams for the implementation of functions: a) $\mathrm{sgn}(\widetilde{X}_1)$; b)-c) $|\widetilde{X}_1|$, $|\widetilde{X}_4|$.

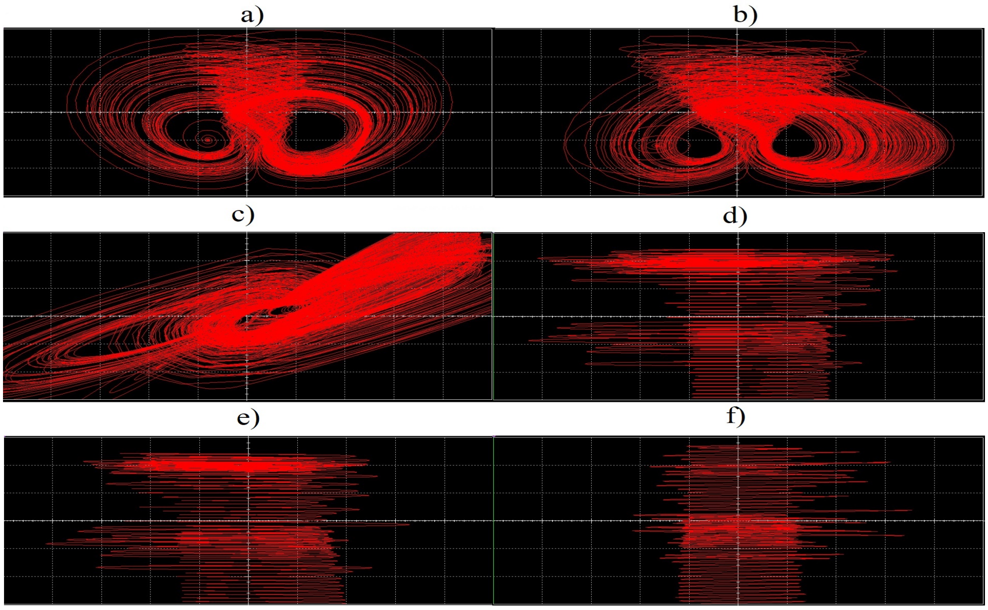

Figure 10: Phase portraits of the new 4D hyperchaotic system as generated in Multisim oscilloscopes: a) $\widetilde{X}_1\widetilde{X}_3$, b) $\widetilde{X}_2\widetilde{X}_3$, c) $\widetilde{X}_1\widetilde{X}_2$, d) $\widetilde{X}_1\widetilde{X}_4$, e) $\widetilde{X}_2\widetilde{X}_4$, f) $\widetilde{X}_3\widetilde{X}_4$.

hidden attractors. With two positive Lyapunov exponents, it is classified as hyperchaotic, and its Kaplan-Yorke dimension ($D_{KY} = 3.3919$) highlights its complexity. Simulation results from the electronic circuit of the proposed 4D system, designed in Multisim 14, align well with those obtained in Mathematica.

The new system shows great potential for applications in encrypting and decrypting information signals, images, data for the Internet of Things, and similar areas.

Acknowledgment

The author is grateful to the editor and reviewers for their interest in the paper and valuable comments.

References

[1] L. O. Chua. Memristor – the missing circuit element. *IEEE Transactions on Circuit Theory* **18** (5) (1971) 507–519.

[2] D. B. Strukov, G. S. Snider, D. R. Stewart, and R. S. Williams. The missing memristor found. *Nature* **453** (2008) 80–83.

[3] O. Krestinskaya, A. James, L. O. Chua. Neuro-memristive circuits for edge computing: a review. *IEEE Transactions on Neural Networks and Learning Systems* **31** (2020) 4–23.

[4] A. G. Radwan, M. E. Fouda. *On the Mathematical Modeling of Memristor, Memcapacitor and Meminductor*. Springer Cham, 2015. https://doi.org/10.1007/978-3-319-17491-4

[5] G. A. Leonov, N. V. Kuznetsov and V. I. Vagaitsev. Localization of hidden Chia's attractors. *Physics Letters A* **375** (23) (2011) 2230–2233.

[6] S. F. Al-Azzawi, Anmar M. Hasan. A New 4D Hidden Hyperchaotic System with Higher Largest Lyapunov exponent and its Synchronization. *International Journal of Mathematics, Statistics and Computer Science* **2** (2024) 63–74.

[7] A. Sambas, S. Vaidyanathan, S. F. Al-Azzawi, M. K. M. Nawawi, M. A. Mohamed, Z. A. Zakaria, S. S. Abas and M. Mamat. Modelling and MultiSim Simulation of a New Hyperchaos System with No Equilibrium Point. *Nonlinear Dynamics and Systems Theory* **23** (4) (2023) 422–433.

[8] V. T. Pham, C. Volos, L. V. Gambuzza. A memristive hyperchaotic system without equilibrium. *Scientific World Journal* **2014** (2014) 368986.

[9] K. Rajagopal, A. Bayani, A. J. M. Khalaf, H. Namazi, S. Jafari and V. T. Pham. A no-equilibrium memristive system with four-wing hyperchaotic attractor. *International Journal of Electronics and Communications (AEU)* **95** (2018) 207–215.

[10] P. P. Singh, B. K. Roy, C. Volos. Chapter 9 – Memristor-based novel 4D chaotic system without equilibria. Editors: Christos Volos, Viet-Thanh Pham. In: Advances in Nonlinear Dynamics and Chaos (ANDC), Mem-elements for Neuromorphic Circuits with Artificial Intelligence Applications. Academic Press, 2021, Pages 183–205. https://doi.org/10.1016/B978-0-12-821184-7.00017-7.

[11] V. K. Tamba, F. K. Tagne, A. L. M. Biamou, M. C. Nkeing and A. N. Takougang. Chapter 7 – Hidden extreme multistability generated from a novel memristive two-scroll chaotic system. Editors: Christos Volos, Viet-Thanh Pham. In: Advances in Nonlinear Dynamics and Chaos (ANDC), Mem-elements for Neuromorphic Circuits with Artificial Intelligence Applications, Academic Press, 2021, Pages 147–164. https://doi.org/10.1016/B978-0-12-821184-7.00015-3.

[12] A. Irfan. Simple chaotic jerk, hyperjerk, and hyperchaotic hyperjerk circuits and systems: families of self-excited and hidden attractors. Thesis PhD. 2020. https://doi.org/10.14457/TU.the.2020.75.

[13] A. S. Elwakil, S. Ozoguz and M. P. Kennedy. Creation of a complex butterfly attractor using a novel Lorenz-Type system. *IEEE Transactions on Circuits and Systems I: Fundamental Theory and Applications* **49** (4) (2002) 527–530.

[14] H. Binous and N. Zakia. An Improved Method for Lyapunov Exponents Computation. https://library.wolfram.com/infocenter/MathSource/7109/, March 09, 2008.

[15] X. Liu, X. Y. Zhang, P. Li and H. Yan. A new Lorentz chaotic system and its circuit implementation. Proceedings of the 8th EAI International Conference on Green Energy and Networking, GreeNets 2021, June 6–7, 2021, Dalian, People's Republic of China, 2021, https://api.semanticscholar.org/CorpusID:239146374.